ADSORPTION OF HEAVY METALS FROM WATER USING *MORINGA OLIFERA* PODS MODIFIED WITH IRON OXIDE NANOPARTICLES

Mokete Phele[1, 2], Fanyana Mtunzi[1, 2], David Shooto[2]

[1]Department of Chemistry, Faculty of Applied and Computer Sciences, Vaal University of Technology, Vanderbijlpark, 1911, South Africa, phelemj85@gmail.com
[2]Institute of Chemical and Biotechnology, Faculty of Applied and Computer Sciences, Vaal University of Technology Southern Gauteng Science and Technology Park, Sebokeng, 1983, South Africa

ORIGINAL SCIENTIFIC PAPER

ISSN 2637-2150
e-ISSN 2637-2614
UDC 504.43.054:669.018.674
DOI 10.7251/STEDZ2402039P
COBISS.RS-ID 141779713

Received: *22 October 2024.*
Accepted: *23 November 2024.*
Published: *29 November 2024.*
http://stedj-univerzitetpim.com

Corresponding Author:
Mokete Phele, Department of Biotechnology and Chemistry, Faculty of Applied and Computer Sciences, Vaal University of Technology, Vanderbijlpark, 1911, South Africa, phelemj85@gmail.com

Citation:
Phele, M., Mtunzi, F., & Shooto, D. (2024.). Adsorption of heavy metals from water using *Moringa Oleifera* pods modified with iron oxide nanoparticles. *STED Journal, 6*(2), 39-52.

ABSTRACT

The adsorption process by metal oxide nanoparticles has been investigated an effective agent for removing organic and inorganic contaminants from water and wastewater. In this study, iron oxide nanoparticles were synthesized in the presence of *moringa oliefera* pods as adsorbent for lead, copper and cadmium ions adsorption. *Moringa oliefera* pods biochar with Fe_3O_4 particles precipitated on the surface of biochar was synthetized by co-precipitation method. Batch adsorption method was used, and heavy metal ions percentage recovery was measured using ICP-OES. Effect of various parameters such as contact time, pH, metal concentration and adsorbent dosage was determined on the removal efficiency. The maximum adsorption capacities of Pb^{2+}, Cd^{2+}, and Cu^{2+} by MMC were 31.46 $mg{\cdot}g^{-1}$, 29.05 $mg{\cdot}g^{-1}$ and 27.66 $mg{\cdot}g^{-1}$, respectively. The Langmuir and Freundlich isotherm equations were used to analyze the equilibrium isotherm data. The adsorption process fit the second-order kinetics well in all cases, and the Langmuir isotherm equation fit the experimental data well.

Keywords: *Moringa Oleifera*, iron oxide nanoparticles, co-precipitation, adsorption

INTRODUCTION

Water is an essential element for the sustainability and development of life on Earth. An average person requires around 50 liters of water per day, to fulfil their biological needs and domestic activities (Howard, & Bartman, 2003). To guarantee access to safe drinking water is a political concern at national, provincial and local levels. It ensures

the health safety of the population, given that, the lack of it promotes the proliferation of diseases (World Health Organization [WHO], 2017). Children and young people are the most vulnerable to get water-related diseases like diarrhea, trachoma, schistosomiasis and other diseases, preventable diseases (Howard, & Bartman, 2003) which due to the absence of drinking water and suitable sanitation, nowadays are the cause of 2 million to 5 million deaths per year (World Health Organization [WHO], & United Nations Children's Fund [UNICEF], 2000). The Earth is mostly constituted by water, covering almost 70 % of it. However, 96.5 % of the hydrosphere is saline water from the oceans and just 2.5 percent is freshwater which, around 68 % of it is enclosed in ice caps, glaciers and snow (Shiklomanov, 2003, pp 13-23; Mushtaq, Singh, Bhat, Dervash, & Hameed, 2020, pp 27-50).

Freshwater complies an important role in preserving life, how it is used and dispose of is an environmental issue of international concern (Gleick, 2003). Especially, due to the high level of water's vulnerability to contamination (Mushtaq, et al., 2020, pp 27-50), which can be polluted by different sources as microbial, chemical, physical or biotic factors (WHO, 2017). The main reason for water pollution is due to anthropogenic activities, and the rapid increase in human population makes the situation even worse (Gleick, 2003). Overcrowded areas, industrial activities, discharge of fields, production and use of plastic, chemicals, debris, etc., are just a few examples of the damage to the planet's sources of water (Mushtaq, et al., 2020, pp 27-50).

Several water-treatment technologies are now being combined around the world, taking into account various elements such as population, implementation and maintenance costs, and community behaviour to assure the system's long-term success (United Nations Educational, Scientific and Cultural Organization [UNESCO], 2009). Depending on the scope of the system, it can be applied at home or for a whole community. For household water treatment, there are three main methods: boiling the water, slow sand filter, and domestic chlorination. While, for a community, there are other options like: storage and sedimentation, up-flow roughing filter, complete water treatment plants and chlorination in piped water-supply systems (Trösch, 2009, pp 394–397). Despite the efforts to provide access to drinking water and sanitation to all nations, new threats are found during the process, such as economic troubles, lack of workforce or human resources, minimum political interest, absence of access roads, etc (WHO & UNICEF, 2000). Thus, there are numerous communities around the world without access to drinking water waiting for a solution to their hard reality (Howard, & Bartman, 2003). Scientific research suggests the possibility of using natural technologies, such as: soil filters, treatment wetlands, aerobic and anaerobic treatments, as the first solution to this matter (Rozkošný, Kriška, Šálek, Bodík, & Istenič, 2014). However, the search for natural, replicable and accessible options is still being pursuit.

With the aforementioned in mind, the objective of this study was to develop an efficient magnetic compound adsorbent from *Moringa Oilefera* pod readily available. The magnetic compound adsorbent will then be utilized for the removal of inorganic (Cd^{2+}, Pb^{2+} & Cu^{2+}) cationic pollutants, and the experimental data described using kinetic and adsorption isotherm models.

EXPERIMENTAL

Material and Methods

Collection and Preparation of *Moringa Oleifera* Pods

Moringa oleifera pods were collected from trees in Limpopo farm near Polokwane. Soon after collection, pods were washed thoroughly with doubly distilled deionized water to remove water soluble impurities and oven dried at 105°C for 24 hours. The washed and dried material was pulverized (by mortar and pestle) and sieved to different mesh sizes. The sieved material was rewashed thoroughly with doubly distilled deionized water to remove the fine particles and dried at 105°C for 4 hours. The material was treated with 0.1M nitric acid and methanol for 4 hours to

remove inorganic and organic matter from the sorbent surface and dried in an electric furnace. The treated and untreated materials were then placed in a desiccator to be used as sorbents.

Batch biosorption experiments were conducted to investigate the influence of physiochemical parameters such as contact time, metal ion concentration, adsorbent dosage, and temperature on heavy metals ion adsorption. Batch experiments were performed for different metal concentrations (20 - 100 mg. L^{-1}), temperature (20 - 60°C), adsorbent dose (0.25 - 1.0 g) and contact time (0 - 60 min). After prescribed contact time, the solution was filtrated using filter syringe and the concentration of metal in the filtrate was measured using atomic adsorption spectroscopy.

Preparation of the iron oxide magnetic nanoparticles, biochar, and composite

The Fe_3O_4 magnetic nanoparticles (MNP) was prepared from a 400mL solution of $FeCl_3$ (7.8 g, 28 mmol) and $FeSO_4$ (3.9 g, 14 mmol) at room temperature using the chemical co-precipitation method (Oliveira, et al., 2003). The solution was continuously stirred with an overhead stirrer while 1.0M NaOH solution was added drop-wise to precipitate the MNP. The MNP was magnetically separated, washed with water and then ethanol before drying. The mass of MNP after drying was noted.

The pulverized *moringa* pods (PMP) was separately charred in a crucible at 250°C for 4 hours to obtain the *moringa* biochar (MBC). The biomass was first dried at 110°C for 1 hour before increasing the temperature at a rate of 5°C /min until 250°C which was maintained for 4 hours. The PBC was then cooled, ground, sieved through a 230 mm mesh size sieve. This was followed by washing until the filtrate was colourless indicating no leaching of residual Fe or carbon. The MBC was again dried at 105°C for 2 hours, cooled, weighed noted, and stored.

The MBC-MNP combo (MMC) was prepared by calcining the treated *moringa* pods (MOP) and MNP. The MNP was prepared by chemical co-precipitation in the presence of the treated MOP and subsequently calcining at 250°C. Typically, the MOP was suspended in a 400 mL solution of $FeCl_3$ (7.8 g) and $FeSO_4$ (3.9 g) and stirred thoroughly to allow for wetness. A solution of 1.0M NaOH solution was added drop-wise to raise suspension pH to 10 and precipitate the MNP on the MOP surface. The solution was further stirred for 30 min before separation by centrifugation at 2500 rpm for 4 min. followed by filling of the residue into a crucible for the calcining process. The crucible was heated at 110°C for 1 hour before raising the temperature at a rate of 5°C/min until 250°C which stood for 4 h. After the calcining process, the MMC combo was cooled and washed with water until the filtrate was colourless indicating no leaching of organic matter or iron. The MMC was subsequently dried at 105°C for 2 hours and stored.

Data Management

Adsorption capacity (mg. g^{-1}) at equilibrium for adsorption of analyte were determined by equation 1.

$$q_e = \frac{(C_0 - C_e)}{M} V \qquad 1$$

where C_o and C_e are the initial and final pollutant concentrations (mg. L^{-1}), respectively, while M (mg) and V (mL) are the MMC mass and solution volume, respectively.

Adsorption Isotherm of MMC

Langmuir and Freundlich adsorption isotherm models were used to depict the equilibrium between adsorbed Pb^{2+}, Cd^{2+} and Cu^{2+} on MMC (q_e) and ions concentration in solution (C_e) at constant temperature (30 °C).

Kinetic Study of MMC

The pseudo-first order and pseudo-second order kinetic models were used to describe the adsorption process.

Thermodynamic Parameters

Thermodynamic parameters such as *Gibbs free energy* (ΔG), *enthalpy* (ΔH) and *entropy* (ΔS) for the adsorption of cations on

PILC are calculated using the following equations (Airoldi, Machado, & Lazarin, 2006; Guerra, Lemos, Airoldi, & Angelica, 2006):

$$\Delta G = -RT\ InK_L \qquad 2$$

where K_L is the equilibrium constant obtained from Langmuir model, T the absolute temperature (K) and the universal gas constant R=8.314×10^{-3} kJK^{-1}mol^{-1}. The relationship between K and thermodynamic parameters of ΔH and ΔS can be described by the Van't Hoff correlation in the following equation (Celik, & Ozdemir, 2018; Yildiz, Erol, Aktas, & Alimli, 2004):

$$InK = \frac{\Delta S}{R} - \frac{\Delta H}{RT} \qquad 3$$

The thermodynamic study was made at three different levels of temperatures which were 25, 40 and 70 °C.

RESULTS

Fourier Transform Infrared Spectroscopy (FTIR)

The main functional groups present in the *M. oleifera* pods were characterized by infrared material analysis. The FTIR, one can confirm the potential applicability of adsorption of different pollutants on *M. oleifera* with sufficient and satisfactory removal efficiency. As shown in Figure 1(a-b), the FTIR spectroscopic analysis indicated broad band at 3326 cm^{-1}, representing bonded – OH groups. The band observed at 2917–2849 cm^{-1} was assigned to the aliphatic C–H group. The peak around 1623 cm^{-1} corresponds to C=O stretch. The peak observed at 1541 cm^{-1} corresponds to the secondary amine group, while the peak at 1374 cm^{-1} corresponds to the symmetric bending of CH_3; the one observed at 1314 cm^{-1} corresponds to the C–H bending. Also, the peak observed at 1242 cm^{-1} corresponds to the –SO_3 stretching, at 1029 cm^{-1} corresponds to C=O bonds of ether, ester or phenol, at 668 cm^{-1} corresponds to –CN stretching, while the peak observed at 564 cm^{-1} corresponds to S–O. On the other hand, typical functional groups for iron oxide are depicted by absorption band at 3660 cm^{-1} that corresponds to the hydroxyl functional group and a band obtained at 531 cm^{-1} is characteristic of $M_{tetrahedral}$ resonance with O. This peak also relates to Fe-O group. These results are in confirmation with the study by: (Amuanyena, Kandawa-Schulz, & Kwaambwa, 2019).

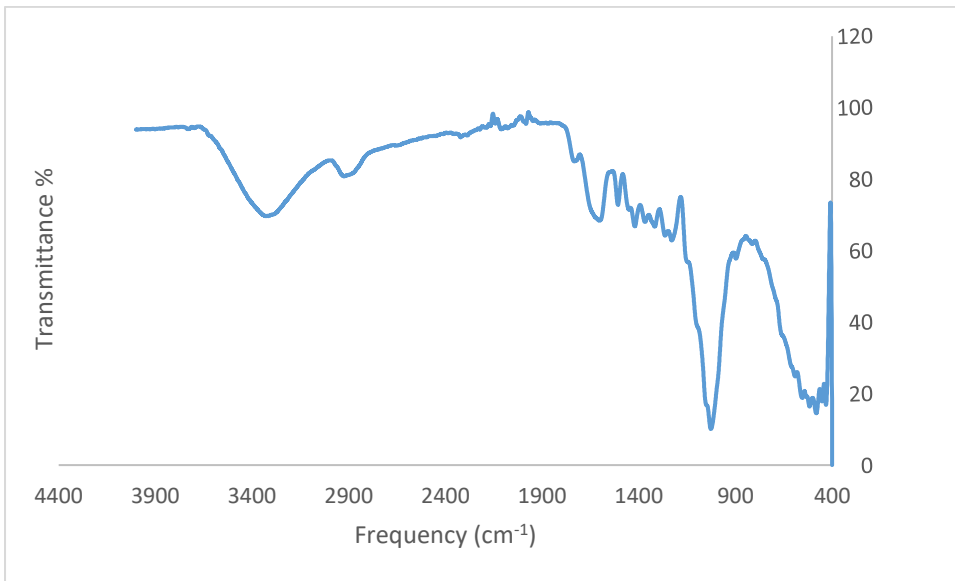

Figure 1a: FT-IR spectrum of *moringa oleifera* pods.

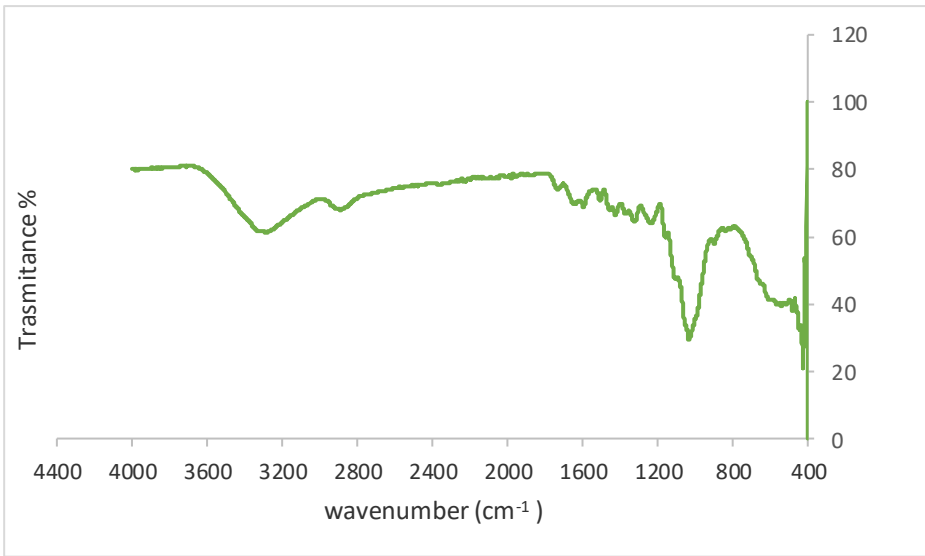

Figure 1b: FT-IR spectrum of magnetic *moringa oleifera* pods.

Scanning electron microscope (SEM)

The SEM images (Figure 2a-b) were evaluated to study the surface morphology of the adsorbents before adsorption of the cations. The SEM images of the *M. oliefera* pods biomass were foamy and fibre-like in nature with no particular shape as reported elsewhere (Tavengwa, Cukrowska, & Chimuka, 2016). However, after the thermal treatment (250°C) the surface morphology revealed macropores and irregular trough-like patterns. The structure appeared frail and the cell morphology of plant biochar was absent. The micrographs of *moringa* pods (Figure 2(a)) reveal mesoporous structures with different pore sizes. These surface characteristics would result in high metal binding due to available binding cavities for the metal ions (Araujo, et al., 2010; Maina, Obuseng, & Nareetsile, 2016). The porosity for the magnetic *moringa* composite has improved compared to the modified *moringa* pods. This may therefore explain the difference in the adsorption capacity of metal ions using these adsorbents. As also shown, the magnetite composite seems to have agglomerated and this could be attributed to strong bonding of nanoparticles, magnetic dipoles as well as Van der Wall forces (Ehrampoush, Miria, Salmani, & Mahvi, 2015; Rajput, Pittman, & Mohan, 2016).

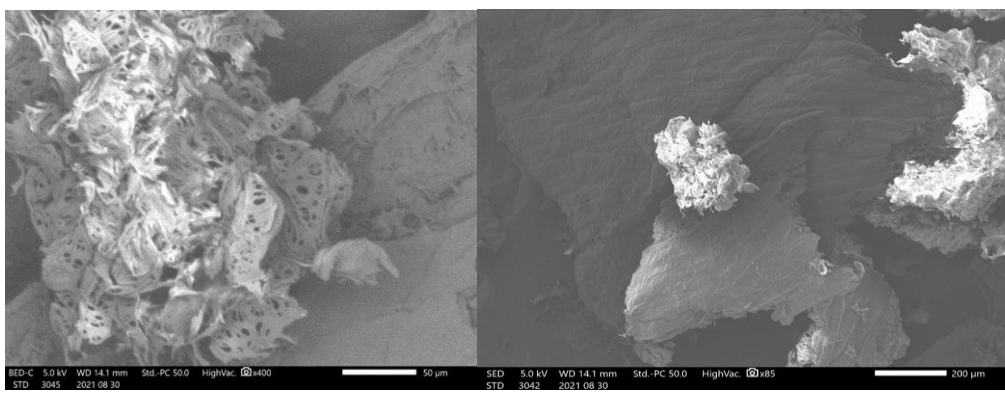

Figure 2: SEM images: (a). MOP before adsorption, (b). MMC before adsorption

Thermogravimetric analysis (TGA)

Thermal stability of MMC was studied when MMC was heated from 20, 50˚C to 80˚C as shown in Figure 3. The different thermal decomposition stages in terms of percentage weight loss and their respective derivatives weight loss percentage per ˚C were obtained by: (Araujo, et al., 2010). The first stage between 20˚C to 100˚C is associated with water loss. The second stage ranging from 100˚C to 350˚C could be due to loss of organic matter that might include proteins amino acid residues with various functional groups and other low molecular weight compounds. The third stage between 350˚C to 780˚C might be from compounds with higher boiling point. At the end of the decomposition stage (780˚C), the total residue was therefore attained.

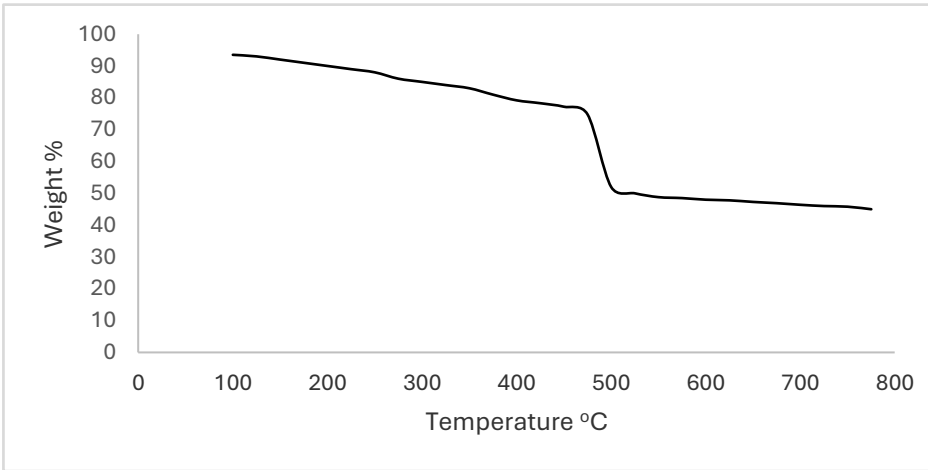

Figure 3: TGA curve for MMC

Effect of contact time

The effect of contact time is shown in Figure 4, indicates the biosorption capacity of MMC for heavy metal ions and it was investigated for various initial concentration 20 - 100 mg. L^{-1} at temperature 25°C, with a fixed adsorbent dose 0.25 - 1 g at interval of 10 min. From the obtained results, it is observed that the percentage of removal of heavy metal ions increases sharply with contact time in the first 10 min. This is due to the presence of large number of vacant sites. As the time proceeds, the removal decreases due to the accumulation of metal ions on the vacant sites until it approaches equilibrium. A study by Maina, et al. (2016) explained further that increase in percentage recoveries with increase in adsorbent dosage is observed until an optimal adsorption level is attained after which the percentage recoveries are reduced due to the decline in vacant active sites on the surface of the adsorbent. Therefore, further increase in contact time did not enhance the biosorption removal, and the optimum contact time within 60 min for lead, copper and cadmium as shown in Figure 4, after that a maximum removal is attained.

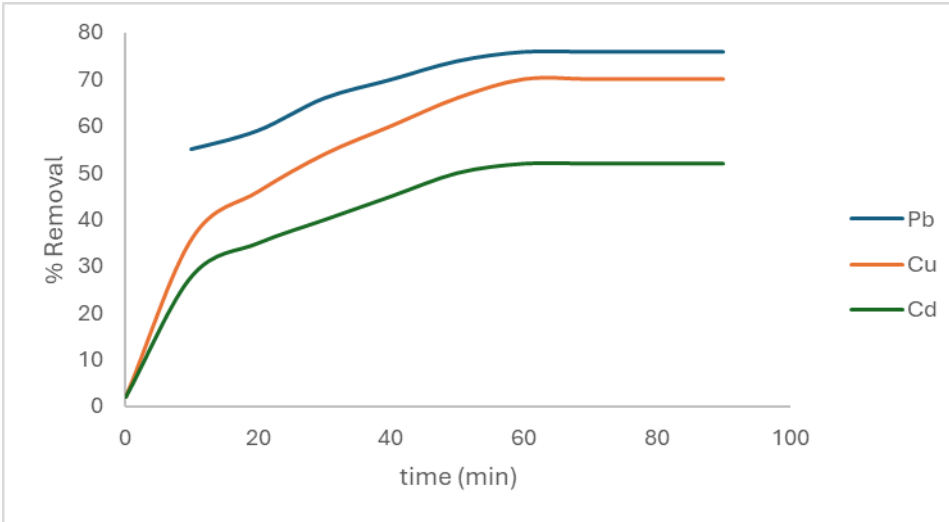

Figure 4: Effects of contact time

Effect of pH

The pH of solution has been identified as the most important variable affecting metal adsorption onto adsorbent. This is partly because hydrogen ions themselves are strongly competing with adsorbate. The removal of Pb^{2+} as a function of hydrogen ion concentration was examined at pH 2 - 9. The removal efficiency was found to be highly dependent on hydrogen ion concentration of solution. The effect of pH on adsorption efficiency is shown in Figure 5. The cadmium ions are usually soluble in acidic pH and the maximum removal of cadmium was obtained in the pH of 4.

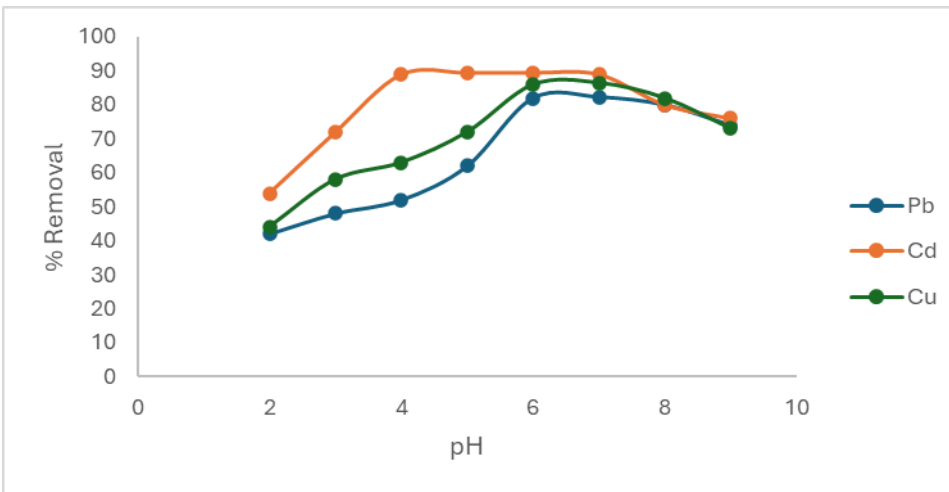

Figure 5: Effects of pH

Effect of biosorbent dose

The adsorption process is affected by adsorbent dose of the aqueous solution. It is clear that the biosorbent dosage parameter plays an important role on the adsorption process. To achieve maximum biosorption capacity, the optimum dosage of MMC must be determined. In such, different amounts of MMC have been used, varying from 0.25 to 1 g of solution with 20 - 100 mg. L^{-1} concentration of heavy metals with temperature kept at 25°C. The effect of adsorbent dose on heavy metal removal is shown in Figure 6. Obviously, the adsorption increased as the sorbent dose of MMC increased. It is elaborated that maximum biosorption attained at biosorbent dosage 1 g is 82, 90 and 92% for Pb^{2+}, Cu^{2+} & Cd^{2+}, respectively, as shown in Figure 6.

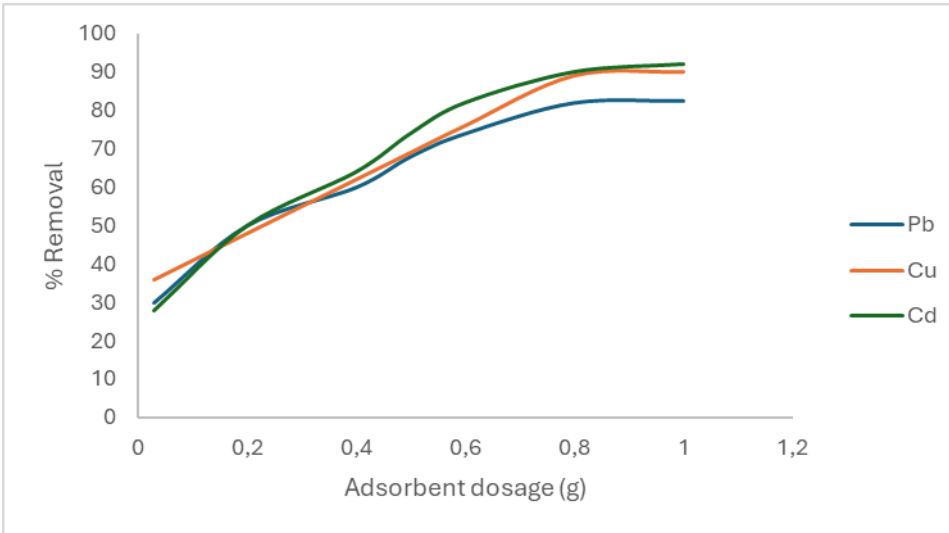

Figure 6: Effect of adsorbent dosage

Effect of temperature

To study the effect of temperature on the amount of uptake of metal ions, the adsorption process was investigated at three different temperatures 25, 40 and 70°C with concentrations of 25 - 100 mg. L^{-1} and constant adsorbent doses 0.25 - 1.00 g. According to Figure 7 the amount of adsorption capacity decreases with the increase of temperature for copper and cadmium. Also, reveals that the lead ions' removal occurs in an exothermic way, once the temperature increases, there is a tendency of reducing lead removal percentage. Thus, the optimal temperature for the removal is at 25°C. Regarding the exothermic characteristic of biosorption, where the process is favoured at low temperatures, (Nordine, et al., 2014), in their work on lead biosorption by pine and sawdust, concluded that the increase in temperature may be causing the destruction and solubilisation of the adsorption sites, thus justifying the lowest percentage of removal obtained by raising the temperature.

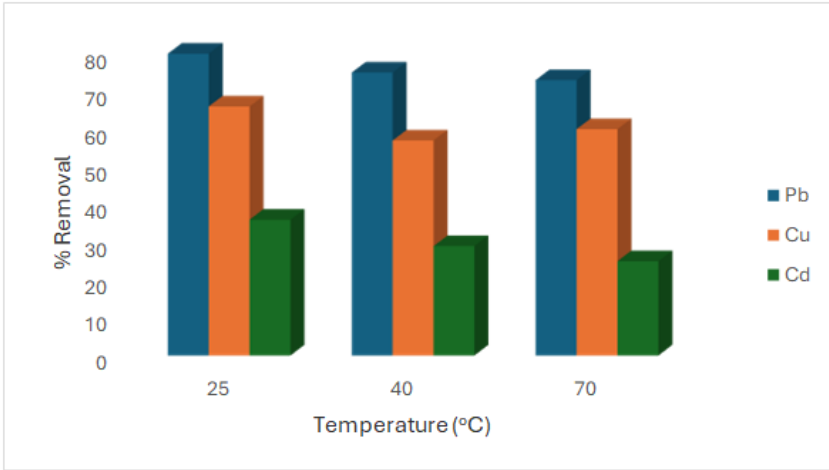

Figure 7: Effect of temperature

Initial metal concentration

As the initial concentration for metal ions increases, the removal percentage decreases for a fixed adsorbent dose and contact time. This behaviour can be explained due to limited active site on the adsorbent surface. The results as depicted in Figure 8, show one example for copper, lead and cadmium ions removal at different concentration and at 25°C. This figure reveals that the amount of metal ions adsorbed per unit mass of adsorbent increase with increasing in concentration from 20 to 100 mg. L^{-1}. At higher concentration, the numbers of metal ions are relatively higher than the available sites, hence, decreasing the removal percentage. Whereas, increasing the biosorbent dose yields to more active sites, which enhance the metal ions uptake. However, further increase in mass for certain metal ions did not bring any further improvement in the removal percentage. With each increasing metal ion concentration, there was an increase in the amount of metal ion adsorbed due to increasing driving force of the metal ions toward the active sites on the adsorbents (Obuseng, Nareetsile, & Kwaambwa, 2012), but the percentage of ions remaining in the solution also increased because of the increscent initial concentration. It indicated a decrease in the active sites on the sorbent as more metal ions were adsorbed.

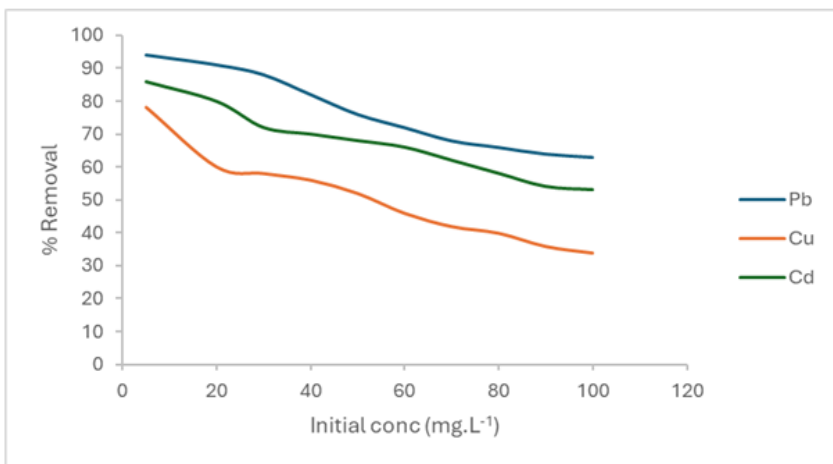

Figure 8: Effect of the initial concentration

Kinetic study

The kinetic studies and modelling of the experimental data are presented in Figure 9 and certain parameters are shown in Table 1. From the correlation coefficient obtained as presented in Table 1 for the pseudo-first-order and pseudo-second order models, it is verified that both models fit well to the experimental data. The pseudo-second-order model proposed by (Ho, Wase, & Forster, 1996) assumes that the process occurs by chemical adsorption involving the participation of valence forces or electron exchange between the metal and the biosorbent, while the pseudo-first-order model assumes the occurrence of the adsorption by physisorption.

In this study, the highest correlation coefficient was obtained for the kinetic model of pseudo-second-order, which is the model that best adapts to the experimental data. A preliminary comparison related to adsorption velocity (q_e) between the calculated and experimental values can be performed to prove the best fit, since the values calculated by the kinetic model of pseudo-second-order are closer to those obtained experimentally.

Table 1. Obtained parameters of kinetics models for adsorption on MMC

Ion	Pseudo-first-order				Pseudo-second-order			
	k_1	$q_{e.cal}$	$q_{e.exp}$	R^2	k_2	$q_{e.cal}$	$q_{e.exp}$	R^2
Pb	1.01	38.61	39.10	0.9960	8.53	39.18	39.10	0.9995
Cu	0.58	37.07	38.41	0.9716	2.98	38.73	38.41	0.9961
Cd	1.08	37.98	38.79	0.9931	9.27	38.74	38.79	0.9989

The biosorption rate constant obtained by the pseudo-2nd order has a higher sorption rate for Cd^{2+}, while the Cu^{2+} has lower rate. The values for the rate constants ranged from 2.98 to 9.27 mg. g^{-1} min^{-1}.

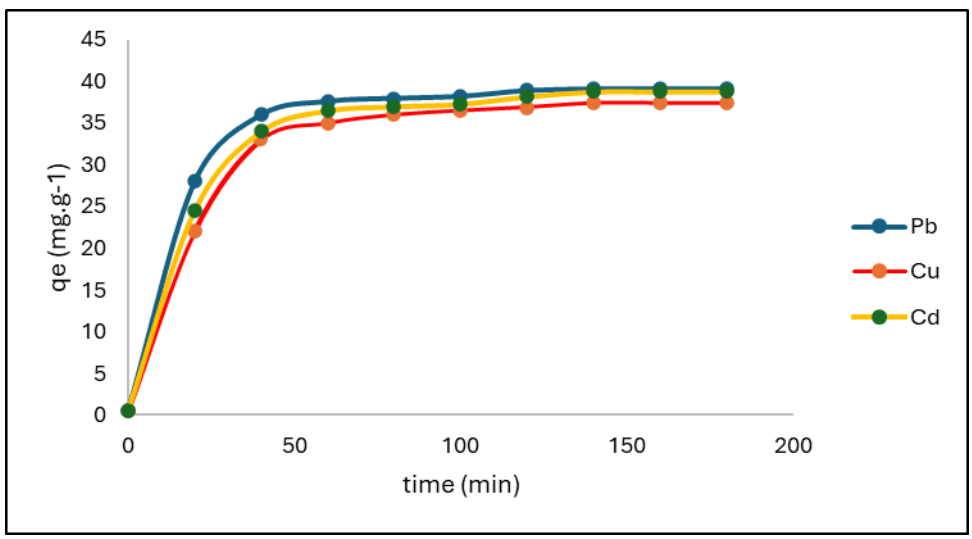

Figure 9: Pseudo-second-order kinetics model for experimental data.

Adsorption thermodynamics

The values of ΔH° and ΔS° could be calculated from the slope of the curve ln K_d versus 1/T, as shown in Figure 10. The thermodynamic parameters obtained from the lead biosorption process are shown in Table 2.

According to Table 2, thermodynamic parameters (ΔG°, ΔH° and ΔS°) of MMC evaluated presented negative values. According to: (Abdeen, Mohammad, & Mahmoud, 2015), negative ΔG° values obtained in respect of studied temperatures show spontaneous and viability natures of biosorption process for lead, copper and cadmium on MMC. Negative ΔH° values confirm that the process has exothermic nature. Kelleher, et al. explain that negative ΔS° values are associated with an increase in the degree of organization of the system, associated with the adsorbate particles' accommodation in more ordered layers on the surface of the adsorbent. It further indicates that there is no dissociation or increased mobility of the particles on the surface of the adsorbent (Kelleher, O'Callaghan, Leahy, O'Dwyer, & Leahy, 2002).

Table 2. Thermodynamics parameters for Pb, Cu & Cd adsorption by MMC

Ion	ΔG° (kJ mol^{-1})					
	298K	308K	318K	R^2	ΔH°(kJ mol^{-1})	ΔS° (J mol^{-1} K^{-1})
Pb	-10.01	-9.69	-9.20	0.9966	-22.16	-40.56
Cu	-12.60	-10.6	-9.89	0.9901	-53.68	-137.5
Cd	-8.32	-8.31	-8.31	0.9991	-8.78	-1.52

In this study, the calculated entropy is negative, according to: (Acharya, Sahu, Mohanty, & Meikap, 2009), negative ΔS° values suggest the probability of a favourable sorption.

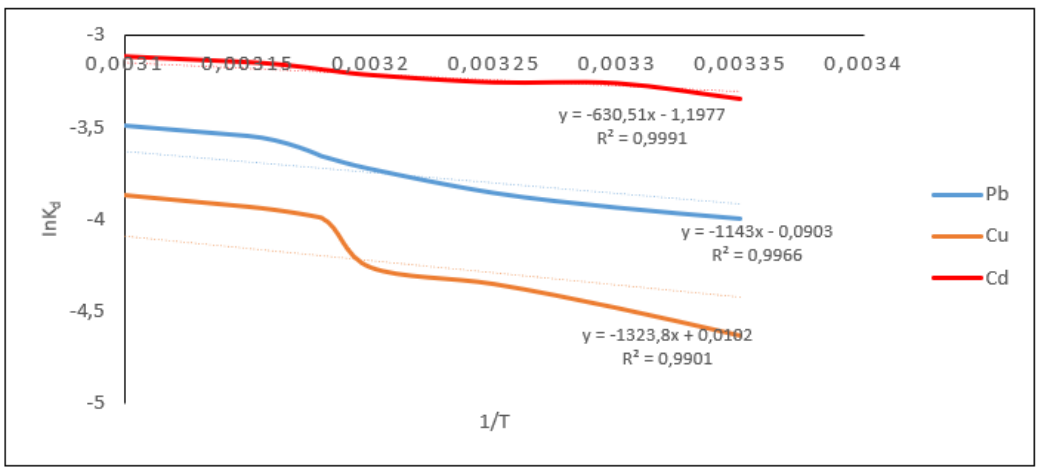

Figure 10: Graph of ln K versus 1/T for the estimation of thermodynamic parameters of biosorption of Pb, Cu & Cd by MMC

Adsorption isotherms

For selecting the optimum operating conditions, the kinetics of metal ions removal was carried out with the help of kinetic models (including pseudo-first order and pseudo-second order models) to investigate the mechanism of sorption and rate controlling steps. The models are fitted to experimental data by nonlinear regression analysis, using coefficient of determination. The preliminary study developed to analyse biosorbents indicated, as optimal conditions for having maximum removal, the use of pH 5.5, contact time 60 min, biosorbent dosage 0.5 g, 50 mL^{-1} and 25°C temperature. Table 3 shows the obtained constants of sorption isotherms for magnetic moringa biosorbents in accordance with the Langmuir and Freundlich models.

Table 3. Langmuir model and Freundlich model parameters**.**

	Langmuir Model			Freundlich Model		
Ions	**q_{max}**	**b**	**R^2**	**k_F**	**n**	**R^2**
Pb^{2+}	31.46	0.21	0.9960	4.09	1.26	0.9863
Cd^{2+}	29.05	0.33	0.9952	1.52	0.39	0.9913
Cu^{2+}	27.66	0.13	0.9968	4.29	1.69	0.9896

From the correlation coefficients (R^2) shown in Table 3, it can be concluded that the Freundlich model does not fit the experimental data, while the model of Langmuir has a good fit. The MMC FTIR spectra showed that metal ions biosorption by moringa seeds occurs, probably, from the chemisorption, in which the chemical interaction between the metal present in the fluid phase and biosorbent was part of the process, resulting, thus, in the transference of electrons equivalent to the formation of chemical bonds between the adsorbate and a solid surface.

CONCLUSION

Various characterization techniques namely, Fourier transform infrared spectroscopy, thermal gravimetric analysis and scanning electron microscope were applied to assess diverse functional groups responsible for adsorption and morphology. The Fourier transform infrared spectroscopy confirmed various functional groups such as amine/amide, carbonyl, hydroxyl, carboxylic and iron oxide on modified magnetic iron oxide nanoparticles that could be responsible for selective recovery of heavy metal ions. Scanning electron microscope depicted porous morphology with various pore sizes that might be responsible for retention of precious metal ions. The optimal conditions for recovery of the heavy metal ions obtained from the study were: pH 6; 60 minutes' agitation time. Furthermore, the experimental data fit the Langmuir and Freundlich models, indicating that the adsorption sites were unequal and non-specific. The findings of the kinetic model fitting revealed that heavy metal ions diffusion and chemisorption processes were limiting the adsorption process. The adsorption process fit the second-order kinetics well in all cases, and the Langmuir isotherm equation fit the experimental data well. The obtained results of this investigation indicated that the synthesized adsorbent was abler to remove heavy metals ions.

REFERENCES

Abdeen, Z., Mohammad, S., & Mahmoud, M. (2015). Adsorption of Mn(II) ion on polyvinyl alcohol/chitosan dry blending from aqueous solution. *Environ Nanotech Monit Manag*, *3*,1-9.

Acharya, J., Sahu, J.N., Mohanty, C.R., & Meikap, B.C. (2009). Removal of lead (II) from wastewater by activated carbon developed from tamarind wood by zinc

chloride activation. *Chem Eng J*, *149*(1), 249-262.

Airoldi, C., Machado, M.O., & Lazarin, A.M. (2006). Thermodynamic features associated with intercalation of some N-alkylmono amines into barium phosphate. *J Chem Thermodyn*, *38*, 130-135.

Amuanyena, M.O.N., Kandawa-Schulz, M., & Kwaambwa, H.M. (2019). Magnetic Iron Oxide Nanoparticles Modified with *Moringa* Seed Proteins for Recovery of Precious Metal Ions. *Journal of Biomaterials and Nanobiotechnology*, *10*, 142-158.

Araujo, C.S.T., Alves, V.N., Rezend, H.C., Almeida, I.L.S., de Assuncao, R.M.N., Tarley, C.R.T., Segatelli, M.G., & Coelho, N.M.M. (2010). Characterization and use of Moringa oleifera seeds as biosorbent for removing metal ions from aqueous effluents. *Wat Sci Tech*, *62*(9), 2198-2203.

Celik, M.S., & Ozdemir, O. (2018). Heterocoagulation of hydrophobized particulates by ionic surfactants. *Physicochem Probl Miner Process*, *54*(1), 124-130.

Ehrampoush, M.H., Miria, M., Salmani, M.H., & Mahvi. A.H. (2015). Cadmium removal from aqueous solution by green synthesis iron oxide nanoparticles with tangerine peel extract. *J Environ Health Sci Eng*, *13*, 1-7.

Gleick, P. H. (2003). Global freshwater resources: soft-path solutions for the 21st century. *Science*, *302*(5650), 1524-1528.

Guerra, D.L., Lemos, V.P., Airoldi, C., & Angélica, R.S. (2006). Influence of the acid activation of pillared smectites from Amazon (Brazil) in adsorption process with butylamine. *Polyhedron*, *25*(15), 2880-2890.

Ho, Y., Wase, D.J., & Forster, C. (1996). Kinetic studies of competitive heavy metal adsorption by sphagnum moss peat. *Environ Technol*, *17*(1),71-77.

Howard, G., & Bartram, J. (2003). *Domestic Water Quantity, Service, Level and Health.* Geneva, Switzerland: World Health Organization.

Kelleher, B.P., O'Callaghan, M.N., Leahy, M.J., O'Dwyer, T.F., & Leahy, J.J. (2002). The use of fly ash from the combustion of poultry litter for the adsorption of chromium (III) from aqueous solution. *J Chem Technol Biotechnol*, *77*(11), 1212-1218.

Maina, I.W., Obuseng, V., & Nareetsile, F. (2016). Use of *Moringa oleifera (Moringa*) seed pods and *Sclerocarya birrea (Morula*) nut shells for removal of heavy metals from waste water and borehole water. *J Chem*, *2016*(1), 9312952, 1-13.

Mushtaq, N., Singh, D.V., Bhat, R.A., Dervash, M.A., Hameed, O.B. (2020). Freshwater Contamination: Sources and Hazards to Aquatic Biota. In: Qadri, H., Bhat, R., Mehmood, M., Dar, G. (Eds.) *Fresh Water Pollution Dynamics and Remediation* (pp 27-50). Singapore: Springer.

Nordine, N., El-Bahri, Z., Sehil, H., Fertout, R.I., Rais, Z, & Bengharez, Z. (2014). Lead removal kinetics from synthetic effluents using Algerian pine, beech and fir sawdust's: optimization and adsorption mechanism. *Appl Water Sci*, *6*(4), 1–10.

Obuseng, V., Nareetsile, F., & Kwaambwa, H.M. (2012). A Study of the Removal of Heavy Metals from Aqueous Solutions by Moringa oleifera Seeds and Amine-Based Ligand 1,4-bis[N, N-bis(2-picoyl) amino)butane]. *Analytica Chimica Acta*, *730*, 87-92.

Oliveira, L.C.A., Rios, R.V.R.A., Fabris, J.D., Sapag, K., Garg, V.K., & Lago, R.M. (2003). Clay-iron oxide magnetic composites for the adsorption of contaminants in water. *Appl Clay Sci*, *22*(4), 169-177.

Rajput, S., Pittman, C.U., & Mohan, J.D. (2016). Magnetic magnetite (Fe_3O_4) nanoparticles synthesis and application for lead (Pb^{2+}) and chromium (Cr^{6+}) removal from water. *J Collo Interf Sci*, *468*, 334-346.

Rozkošný, M., Kriška, M., Šálek, J., Bodík, I., & Istenič, D. (2014). *Natural technologies of wastewater treatment.* Europe: Global Water Partnership Central and Eastern Europe.

Shiklomanov, I.A. (1993). World fresh water resources. In P.H. Gleick (Ed.), *Water in crisis: a guide to the World's Fresh Water Resources* (pp 13–23). Oxford: University Press.

Tavengwa, N.T., Cukrowska, E., Chimuka, L. (2016). Application of raw and biochared Moringa oleifera seed powder for the removal of nitrobenzene from aqueous solutions removal of nitrobenzene from aqueous solutions. *Desalin Water Treat, 57*, 25551-25560.

Trösch, W. (2009). Water treatment. In: Bullinger, H.J. (Eds.) *Technology Guide: Principles - Applications – Trends* (pp 394–397), Berlin, Heidelberg: Springer.

World Health Organization. (2017). *Guidelines for Drinking-water Quality*. Brazil: Interligar,

World Health Organization, & United Nations Children's Fund. (2000). *Global Water Supply and Sanitation Assessment 2000 Report.* USA, Newzork: World Health Organization and United Nations Children's Fund Publications.

United Nations Educational, Scientific and Cultural Organization. (2009). *The United Nations World Water Development Report 3: Water in a Changing World.* Paris, London: UNESCO.

Yildiz, N., Erol, M., Aktas, Z., & Alimli, A.C. (2004). Adsorption of aromatic hydrocarbons on BTEA-betonites. *Adsorpt Sci Technol, 22*, 145-154.